DP-777

AEC RESEARCH AND DEVELOPMENT REPORT

MEASURED LATTICE PARAMETERS FOR NATURAL URANIUM METAL ROD LATTICES IN D_2O

T. J. HURLEY, JR.

This document is furnished pursuant to the Agreement of Understanding of June 7, 1960, between the U. S. and Canadian Governments, establishing a cooperative program on the development of heavy water moderated power reactors.

DUPONT
REG. U.S. PAT. OFF.

Savannah River Laboratory

Aiken, South Carolina

Printed in USA. Price $1.00
Available from the Office of Technical Services
U. S. Department of Commerce
Washington 25, D. C.

DP-777

Physics
(TID-4500, 22nd Ed.)

MEASURED LATTICE PARAMETERS FOR NATURAL URANIUM METAL ROD LATTICES IN D_2O

by

T. J. Hurley, Jr.

Work done by

N. P. Baumann
F. D. Benton
A. E. Dunklee
H. R. Fike
M. R. Fleishman*
M. Raber*
W. E. Graves
T. J. Hurley, Jr.
M. B. Stroud
G. F. O'Neill

August 1963

E. I. DU PONT DE NEMOURS & COMPANY
EXPLOSIVES DEPARTMENT - ATOMIC ENERGY DIVISION
TECHNICAL DIVISION - SAVANNAH RIVER LABORATORY
AIKEN, SOUTH CAROLINA

CONTRACT AT (07-2) - 1 WITH THE
UNITED STATES ATOMIC ENERGY COMMISSION

*On temporary assignment from
United Nuclear Corporation

ABSTRACT

Nuclear parameters of sixteen D_2O-moderated lattices of natural uranium rod clusters were measured in the Process Development Pile. The clusters consisted of 1, 3, 7, or 19 uranium metal rods. Each rod was 1 inch in diameter and was clad with 0.032 inch of aluminum. Triangular lattice spacings between clusters ranged from 7 to 21 inches, center to center. The parameters that were measured included the number of fission neutrons per thermal neutron absorption, η, the fast fission factor, ϵ, the resonance escape probability, p, the thermal utilization, f, and the thermal diffusion area, L^2.

CONTENTS

LIST OF TABLES AND FIGURES

MEASURED LATTICE PARAMETERS FOR NATURAL URANIUM METAL ROD LATTICES IN D_2O

INTRODUCTION

A generalized study of the reactor physics of natural uranium, heavy water systems has been underway at the Savannah River Laboratory. A major feature of the program has been the measurement of bucklings and detailed parameters of lattices of natural uranium metal rod clusters in full-scale critical loadings in the Process Development Pile[1]. The purpose of these experiments was to supply a complete and consistent set of data, over a wide range of lattice spacings and fuel assembly sizes, which could be used to verify methods of calculation. The buckling results from these studies have been reported previously[2]. The measurements of the detailed lattice parameters are the subject of the present report.

SUMMARY

Detailed nuclear parameters (η, ϵ, p, f, and L^2) were measured in the PDP for D_2O-moderated lattices of natural uranium rod clusters. The clusters consisted of 1, 3, 7, or 19 uranium metal rods that were 1 inch in diameter and clad with 0.032-inch aluminum. The lattices were triangular with a pitch (center-to-center spacing between clusters) that ranged from 7 to 21 inches.

The η measurements determined the average number of fission neutrons produced by the absorption of a thermal (subcadmium) neutron in the uranium. They involved comparing subcadmium activations for U^{235} and 1/v foils in the fuel and in a well-thermalized flux. The resultant activity ratios could then be used to adjust the calculated η value for the well-thermalized flux to the values actually prevailing in the fuel. Somewhat unexpectedly the measured η values were almost independent of the fuel cluster size, although as expected they were less than the pure thermal values.

The values of ϵ, the fast fission factor, were determined through measurements of the ratio of U^{238} to U^{235} fissions, δ. These were made by comparing the fission product activities in pairs of natural and depleted uranium foils exposed in the fuel. These ratios were in turn related to the fission ratios on the basis of previously published experiments[9]. As expected, the measured δ (and ϵ) values increased with increasing cluster size but were independent of lattice pitch.

The values of the resonance escape probability, p were deduced from measurements of the ratio of epicadmium to subcadmium neutron capture in U^{238}, ρ. The ρ measurements were made by comparing the γ activity at 103 kev for bare and cadmium-covered foils of depleted uranium that were exposed in the fuel. After correction for extraneous counts, these ratios gave the desired ratio of neutron captures in the $U^{238} \rightarrow U^{239} \rightarrow Np^{239} \rightarrow Pu^{239}$ chain. As expected, the measured ρ values increased with increasing cluster size and with decreasing lattice pitch, and vice versa for the p values.

Thermal neutron disadvantage factors were determined from activation measurements with manganese. These disadvantage factors were then used with the Westcott[5] cross sections in the standard formulas for f and L^2. Results were generally in good agreement with calculations.

The numerical results from these lattice measurements are summarized in Table IX. The definitions of the various parameters as given in the text should be noted before these results are compared with other measurements or calculations. The tabulated numbers range in accuracy from ±0.2% in f to ±3.0% in L^2, the uncertainty in the other parameters is about ±1%. Although the consistency of the data indicates much higher precision than these uncertainties would suggest, a comparison between bucklings calculated from these parameters and the measured bucklings indicates possible systematic errors of this magnitude.

DISCUSSION

GENERAL DESCRIPTION OF THE LATTICES

Fuel pieces for the experiments were assembled from natural uranium metal slugs, 0.998 inch in OD and 8.07 inches long with a density of 18.9 g/cc. The slugs were loaded into air-filled tubes of 1100 aluminum with an ID of 1.026 inches and an OD of 1.090 inches. These tubes were grouped, at a triangular pitch of 1.5 inches center-to-center unless otherwise noted, into clusters of 1, 3, 7, or 19 rods and the clusters hung in triangular lattice arrays in the Process Development Pile (PDP)[1]. Lattice pitches ranged from 7 to 21 inches. For the low buckling lattices a full loading of the PDP was used, while for the higher buckling lattices the outer regions of the pile were poisoned to give an effectively smaller tank diameter. Criticality was controlled by the moderator height. The moderator purity during the experiments ranged from 99.69 to 99.77 mol % D_2O.

THE AVERAGE NUMBER OF FISSION NEUTRONS PRODUCED PER THERMAL ABSORPTION IN THE FUEL

THEORY OF THE MEASUREMENT

The average number, η, of fission neutrons produced by the absorption of a thermal neutron in the fuel is generally given by the following expression

$$\eta(E) = \bar{\nu}/[1 + \alpha(E)] \qquad (1)$$

Here $\bar{\nu}$ is the average number of neutrons produced by a single fission, $1/[1 + \alpha(E)]$ is the fraction of the neutron absorptions in the fuel that lead to fission events, and $\alpha(E)$ is the ratio of the number of capture to fission reactions for neutrons of energy E reacting with the fuel. Although $\bar{\nu}$ is essentially independent of reacting neutron energy in the thermal range, $\alpha(E)$ and hence $\eta(E)$ usually are functions of energy as indicated.

For the purposes of these experiments the thermal cutoff for η was taken equal to the cadmium cutoff. The effect of this assumption is considered in the final section of this report on the comparison of lattice parameters.

Values of $\eta(E)$ for the various fissionable isotopes have been determined in the laboratory, but the application of these results to a particular reactor lattice is doubtful because of the uncertainty in the neutron energy spectrum. Accordingly, an attempt was made to find a method for measuring $\bar{\eta}$ directly in a lattice.

For the natural-uranium-fueled lattices studied in the present experiments, U^{235} is the only isotope fissionable by thermal neutrons, and $\eta(E)$ can be expressed as

$$\eta(E) = \eta^{25}(E) \frac{A^{25}}{A^{25} + A^{28}} \qquad (2)$$

where $\eta^{25}(E)$ is $\eta(E)$ for U^{235} as defined in Equation 1 and $A^{25}/(A^{25} + A^{28})$ is the fraction of the fuel absorptions occurring in U^{235} for neutrons of energy E. If the assumption is made that the neutron energy spectrum in the fuel is very nearly Maxwellian up to the cadmium cutoff at 0.554 ev*, a

*The value obtained using Westcott's[3] formulation for 0.020 inch Cd thickness assuming isotropic flux.

numerical integration of the cross section data given by Hughes[4] shows

$$\eta^{25} \simeq \text{constant} = 2.07 \tag{3}$$

for Maxwellian temperatures from 20°C up to ~300°C. Thus the determination of η reduces to a measure of the fraction of the fuel absorptions of thermal neutrons occurring in U^{235}. Since both A^{25} and A^{28} vary roughly inversely with the neutron velocity, it is permissible to use average values of those quantities in averaging $A^{25}/(A^{25} + A^{28})$ over the thermal neutron energy spectra. Thus from Equation 2 the fractional absorption can be written

$$\frac{A^{25}}{A^{25} + A^{28}} = \frac{1}{1 + \frac{A^{28}}{A^{25}}} = \frac{1}{1 + \frac{A_M^{28}}{A_M^{25}} K} \tag{4}$$

where A_M^{28} and A_M^{25} denote the absorptions in U^{238} and U^{235}, respectively, in a pure Maxwellian spectrum at 20°C and K is a hardening factor given by

$$K = \frac{A^{28}}{A^{25}} \frac{A_M^{25}}{A_M^{28}} \tag{5}$$

The ratio of absorptions* in the pure Maxwellian is

$$\frac{A_M^{28}}{A_M^{25}} = 0.565 \tag{6}$$

So Equation 2 becomes

$$\eta = 2.07(1 + 0.565K)^{-1} \tag{7}$$

where K is to be determined experimentally.

*Cross sections were computed using Westcott's[5] theory and are given in Table I.

TABLE I

Cross Sections and Westcott's g-Factors Used in η Analysis

Parameter	Isotope U^{238}	Isotope U^{235}
σ_a, barns	2.71	667.97
g	1.0017	0.9759

If the hardening term is rewritten as two terms,

$$K = \frac{A^{28}}{A_M^{28}} \frac{A_M^{25}}{A^{25}} \quad (8)$$

K can be determined as the product of two ratios each of which is the ratio of absorptions in the fuel and in a Maxwellian flux.

EXPERIMENTAL PROCEDURE

The experimental measurements of η essentially determined the ratios A^{28}/A_M^{28} and A_M^{25}/A^{25} by comparing foil activations in representative fuel rods with foil activations in a well-thermalized flux. In order to eliminate unnecessary normalizations the fuel and thermal irradiations were made simultaneously. At the wide lattice pitches the reference thermal irradiations were taken in moderator positions at the centroid of three fuel assemblies and at the smaller pitches in moderator positions created by removing a fuel assembly. For both of these positions the thermal neutron energy distribution was assumed to be Maxwellian at the temperature of the moderator.

A description of the measuring foils is given in Table II, while the foil loading in a typical fuel rod is shown in Figure 1. The ratio A_M^{25}/A^{25} was determined directly by comparing the measured activities due to subcadmium U^{235} fissions in the oralloy foils. However the ratio A^{28}/A_M^{28} was determined indirectly. In the thermal region the U^{238} capture cross section is very nearly 1/v and since the subcadmium activations of U^{238} were not readily measurable, the copper and P-metal* foils were substituted as equivalent 1/v detectors. After irradiation all the foils were γ counted with scintillation detectors biased to reject pulses below 0.4 Mev. The recorded activities were corrected for time decay, background, differences in foil weight, and for the relative vertical positions of the foils in the lattice during irradiation. The latter correction was based on the measured vertical (cosine) flux distributions[2].

*P-metal is an alloy of 72% Mn, 18% Cu, and 10% Ni. Under the conditions of the experiment essentially only Mn^{56} activity was counted.

TABLE II

Characteristics of Detecting Foils and Pins

Designation	Material	Size
Cu foil	Natural Cu	1" dia., 0.010" thick
P-metal foil[a]	72% Mn, 18% Cu, 10% Ni	1" dia., 0.005" thick
P-metal pins[a]	72% Mn, 18% Cu, 10% Ni	0.063" dia., 0.5" long
U^{235} foils	7.9 weight % oralloy in Al	1" dia., 0.010" thick
Natural U foil	Natural U metal (0.714% U^{235})	1" dia., 0.006" thick
Depleted U foil	U metal depleted in U^{235} (0.035% U^{235})	1" dia., 0.005" thick

(a) Principal activity is Mn^{56}

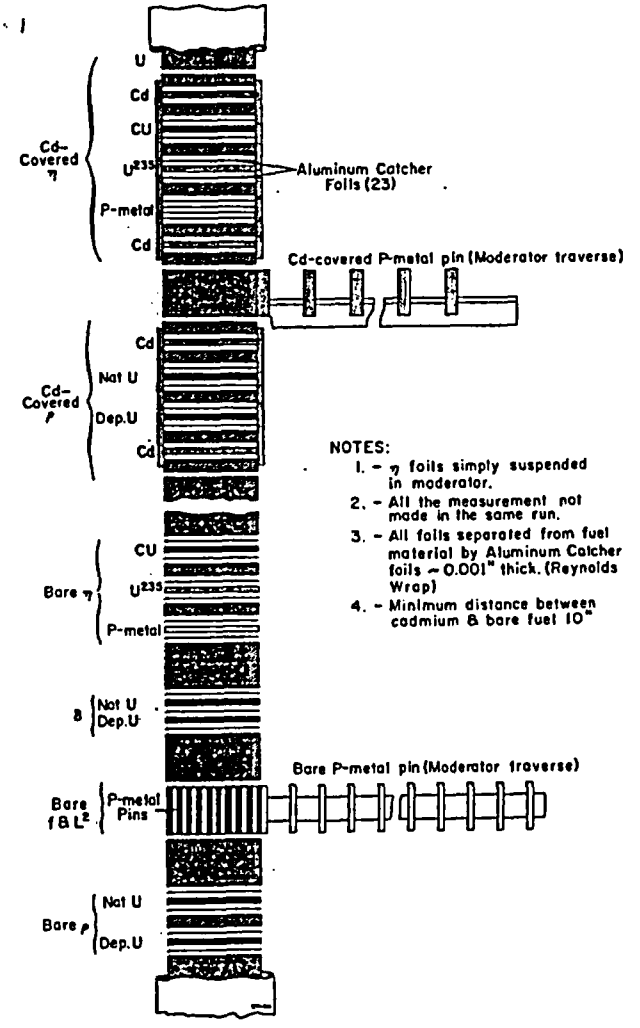

FIG. 1 SCHEMATIC OF TYPICAL FOIL LOADING

From the corrected activities the parameter K_i for each fuel rod was determined by the following expression

$$K_i = \frac{\text{subCd Cu or Mn activity in fuel rod i}}{\text{subCd Cu or Mn activity in moderator}} \times \frac{\text{subCd } U^{235} \text{ activity in moderator}}{\text{subCd } U^{235} \text{ activity in fuel rod i}} \qquad (9)$$

The identification code for the fuel rod positions is shown in Figure 2. The value of K_i for each detector is given in Table III along with the corresponding value of η determined from Equation 7. For the 7- and 19-rod clusters, weighted-average values are also given. The weighting consisted of the normalized product of the number of fuel rods of a particular type and the relative average subcadmium flux in the representative rod.

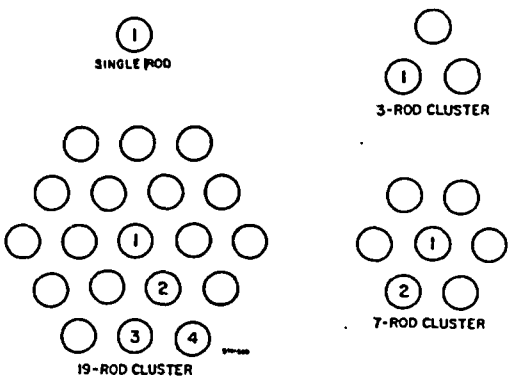

FIG. 2 CROSS SECTIONS OF ROD CLUSTERS
(numbers designate types of fuel rod positions)

TABLE III

Experimental Results of η Measurements

Rods per Cluster	Lattice Pitch, inches	Rod 1[a] R(Cu)	Rod 1[a] R(P-metal)	Rod 1[a] η	Rod 2 R(Cu)	Rod 2 R(P-metal)	Rod 2 η	Rod 3 R(Cu)	Rod 3 R(P-metal)	Rod 3 η	Rod 4 R(Cu)	Rod 4 R(P-metal)	Rod 4 η	$\bar{\eta}$ for Cluster
1	7.00	1.008	1.026	1.312 ±0.015										
	8.08	1.002	1.005	1.318 ±0.013										
	9.33	1.018	1.005	1.315 ±0.013										
	12.12	1.016	1.002	1.318 ±0.013										
3	7.00	1.003	1.006	1.318 ±0.014										
	9.33	1.042	1.020	1.306 ±0.015										
	12.12	1.007	1.014	1.315 ±0.016										
	14.00	1.015	1.006	1.315 ±0.015										
7	9.33	1.031	1.035	1.303 ±0.013	1.022	1.021	1.308 ±0.013							1.308 ±0.016
	12.12	1.026	1.019	1.309 ±0.012	1.024	1.013	1.312 ±0.014							1.311 ±0.018
	14.00	1.049	1.061	1.290 ±0.013	1.040	1.046	1.307 ±0.013							1.306 ±0.016
	18.52	1.019	1.043	1.310 ±0.013	1.007	1.003	1.318 ±0.013							1.317 ±0.016
	21.00	1.006	1.021	1.312 ±0.013	-	-	-							-
7[b]	18.52	1.021	1.036	1.306 ±0.013	1.002	1.021	1.314 ±0.013							1.313 ±0.013
19	14.00	1.074	1.074	1.285 ±0.018	1.138	1.189	1.246 ±0.015	1.052	1.049	1.301 ±0.015	0.955	0.921	1.351 ±0.021	1.311 ±0.024
	18.52	-	-	-	-	-	-	-	-	-	-	-	-	

(a) See Figure 2 for rod number designations

(b) 2.0" center-to-center rod spacing in cluster

RESULTS AND CONCLUSIONS

There is no apparent systematic variation with cluster size or lattice pitch in the η results given in Table III. A simple averaging gives a value of $\eta = 1.310$ with an accuracy of about ±1% for all fuel assemblies studied. This value of $\eta = 1.310$ is to be compared with a value of $\eta = 1.322$ obtained from Equation 7 by setting $K = 1$. Both values are subject to the same assumptions concerning the neutron spectrum, and consequently their difference indicates clearly that some flux hardening occurs in the fuel, but the large uncertainty leaves the magnitude in some doubt. It had been expected that η would get progressively smaller as the fuel cluster increased in size. However, the value of η could in fact be constant for these clusters since the large center-to-center rod spacing creates a fairly dilute fuel bundle and extensive rethermalization could be taking place in the D_2O between fuel rods. The alternative conclusions are that the experiment was not sensitive enough to detect small systematic changes or that the assumptions concerning the spectrum tend to mask the true result. The accuracy of the η determinations is about 1%, estimated from uncertainties in data corrections, counting statistics, and errors in cross sections.

THE FAST FISSION FACTOR

THEORY OF THE MEASUREMENT

The fast fission factor, ϵ, is defined as the ratio of the net number of neutrons produced by all fissions to the number produced by thermal fissions (which here also include epicadmium U^{235} fissions). The fast fission factor for natural uranium can be expressed as

$$\epsilon = 1 + \left(\frac{\nu^{28} - 1}{\nu^{25}}\right)\delta \qquad (10)$$

where ν^{28} and ν^{25} are the numbers of neutrons emitted per fission in U^{238} and U^{235}, respectively; and δ is the ratio of the number of fissions in U^{238} to the number of fissions in U^{235}. This definition differs from the more common one[6] in that it excludes the capture of fast neutrons, which are here included in the resonance escape probability term.

The values of ν^{28} and ν^{25} are fairly well known: $\nu^{28} = 2.85$[7] and $\nu^{25} = 2.43$[8]. Consequently, the experiment is reduced to a determination of δ for each fuel assembly. A complete description of the measurement technique for this determination has been given by Futch[9].

The measurable quantity is $\gamma(t)$, defined as follows,

$$\gamma(t) = \frac{\text{fission product } \gamma \text{ activity/gram in a depleted foil}}{\text{fission product } \gamma \text{ activity/gram in a natural foil}} \quad (11)$$

where activities have been placed on a per-gram basis to account for differences in the foil thicknesses. This quantity is related to δ through the equation[9]

$$\delta = \alpha(t)P(t) \quad (12)$$

The quantity $\alpha(t)$ is given as

$$\alpha(t) = \frac{a\gamma(t) - S}{1 - a\gamma(t)} \quad (13)$$

where $a = N_n^{28}/N_d^{28}$ and $S = (aN_d^{25})/N_n^{25}$ with N^{25} and N^{28} denoting the atom densities of U^{235} and U^{238}, respectively. The subscript n refers to the natural uranium foils and the subcript d to the foils depleted in U^{235}. The factor, P(t), is a previously studied quantity relating the measured foil activity at the time, t, to the number of fissions which occurred in the foils.[9]

EXPERIMENTAL AND ANALYTICAL TECHNIQUES

The quantity $\gamma(t)$ was measured by irradiating pairs of bare natural and depleted uranium foils in representative fuel rods in the configuration shown in Figure 1. To conform to the conditions used for the earlier P(t) calibrations, the foils were irradiated for 30 minutes. They were then γ counted on 2x2-inch NaI(Tl) crystals with the amplifiers biased to accept only pulses with an energy of 1.2 Mev or greater. The purpose of the high bias was to eliminate γ-rays arising from the decay of U^{239} and Np^{239}. The counting order was first a depleted foil, next the associated natural foil, and then the depleted foil again. This process was repeated several times. For each of the three counts an average of the two depleted foil counts gave an effective fission product activity of the depleted foil for the time at which the activity of the natural foil was measured. After corrections for background and the differences in the foil weights, the ratios of these activities gave the desired values of $\gamma(t)$. A second method of analysis was to plot the background and the weight-corrected counts as a function of time for each of the foils. Use of these plots to obtain the $\gamma(t)$ values gave the same results as the first method within the accuracy of the experiment, and the reported values are the average of both methods.

From the description of the measuring foils given in Table II,

$$a \equiv \frac{N_n^{28}}{N_d^{28}} = 0.9932$$

and (14)

$$S \equiv a \frac{N_d^{25}}{N_n^{25}} = 0.0487$$

These values were combined with the measured $\gamma(t)$ values to obtain $\alpha(t)$ according to Equation 13.

The remaining function, $P(t)$, needed to obtain δ from Equation 12 is shown in Figure 3. This particular function was not measured directly but was inferred from the $P(t)$ curve given by Futch[9] and normalized to the 2x2-inch crystals used in these experiments by the measurements by Kinard[10]. The curve has been extrapolated where required to obtain sufficient data for statistical analysis. The extrapolation is believed to be within the combined errors of the work by Futch and Kinard.

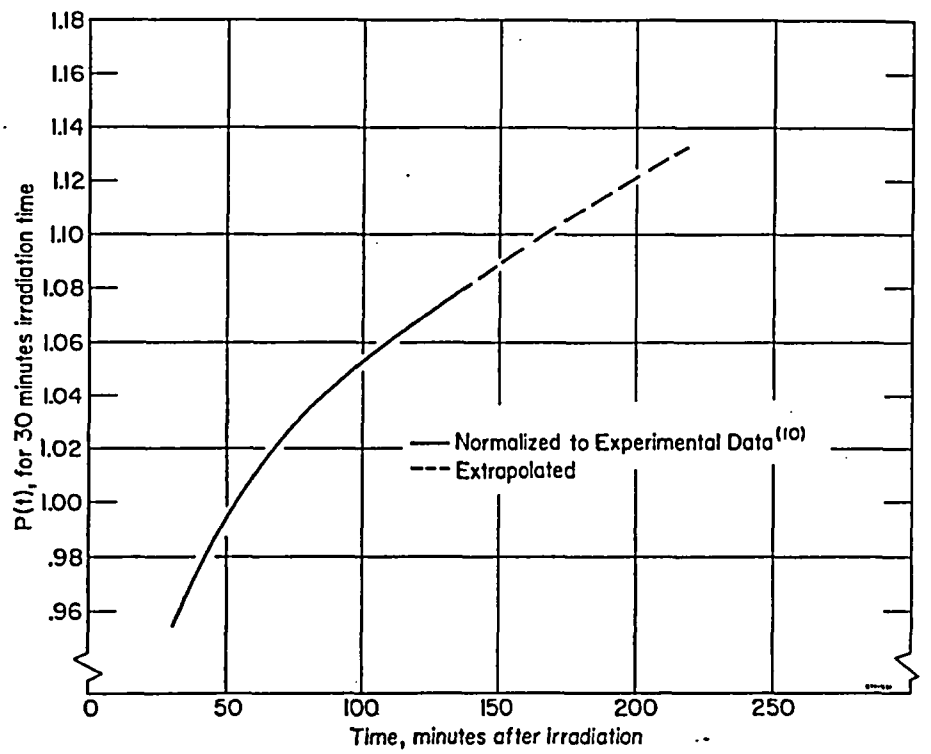

FIG. 3 FUNCTION P(t) VS TIME FOR A 2" x 2" NaI(Tl) WITH A 1/8" Al β SHIELD

RESULTS

The values of δ_1, where i denotes the rod type given in Figure 2, as determined for each representative rod in fuel clusters are given in Table IV. The averaged values of δ for each cluster, also given in the table, were determined by weighting the individual δ's for each rod type by the number of rods of that type in the cluster and by the relative thermal neutron flux level in the rod.

TABLE IV

Experimental Results of Fast Fission Measurements

Rods per Cluster	Lattice Pitch, inches	Individual Rods				Cluster	
		δ_1(a)	δ_2(a)	δ_3(a)	δ_4(a)	δ	ϵ
1	7.00	0.053					
	8.08	0.054					
	9.33	0.050					
	12.12	0.048					
Average for Assembly						0.051 ±0.002	1.039 ±0.002
3	7.00	0.063					
	9.33	-					
	12.12	-					
	14.00	0.062					
Average for Assembly						0.063 ±0.002	1.048 ±0.002
7	9.33	-	-	-	-	-	
	12.12	0.105	0.067			0.071	
	14.00	0.098	0.063	-	-	0.067	
	18.52	0.098	0.066	-	-	0.068	
	21.00	-	-	-	-	-	
Average for Assembly						0.069 ±0.003	1.053 ±0.002
7(b)	18.52	0.074	0.055	-	-	0.057	
Average for Assembly						0.057 ±0.003	1.044 ±0.002
19	14.00	0.179	0.152	0.097	0.075	0.100	
	18.52	0.167	0.142	0.105	0.076	0.102	
Average for Assembly						0.101 ±0.004	1.077 ±0.003

(a) Rod indexing key given in Figure 2
(b) 2.0" center-to-center rod spacing in cluster

The accuracy of these measurements was determined assuming a ±2% deviation due to counting statistics and uncertainties in the isotopic ratios of the foils. An additional ±4% error was assumed in the absolute value of P(t). These values were combined to obtain the assigned uncertainties in δ given in Table IV. The uncertainties quoted for ϵ include only the errors in δ. The uncertainty in the values of ν^{28} and ν^{25}, in addition to the experimental uncertainty, would limit the absolute accuracy of ϵ to the order of ±1%.

The possibility of systematic errors due to the presence of the aluminum catcher foils (see Figure 1) was investigated by a method described by Carter[11], et al. In this method a series of measurements is taken in the same lattice with increasing numbers of the catcher foils. It was determined (in agreement with Carter's results) that the normal catcher foil thicknesses of 0.002 inch or less would not perturb the results.

THERMAL UTILIZATION AND THERMAL DIFFUSION AREA

THEORY OF THE MEASUREMENTS

Thermal Utilization

The thermal utilization, f, is defined as the number of thermal (subcadmium) neutrons absorbed in the fuel per thermal neutron absorbed in the reactor. For the rod clusters under consideration in this report, f may be expressed by the following equation

$$f = \frac{(\bar{\phi} V \Sigma_a)_{fuel}}{\sum_i (\bar{\phi} V \Sigma_a)_i} \qquad (15)$$

where $\bar{\phi}$ = average thermal flux in each material

V = volume of material

Σ_a = averaged macroscopic absorption cross section of the material

i - denotes the material (fuel, moderator, coolant, or cladding)

The purpose of distinguishing the moderator from coolant, since there are no housing tubes, is simply as a matter of convenience in estimating the flux in the D_2O inside a rod cluster, whose area is defined as that enclosed by a rubber band around the cluster.

The volume terms in Equation 15 were measured directly. The effective cross sections were computed (up to the cadmium cutoff) by the S_4 spectrum formulation of Westcott[5] and are given in Table V. In keeping with the definition of η, the thermal cutoff was again defined as the effective cadmium cutoff energy (0.554 ev).

Thermal Diffusion Area

The thermal diffusion area, L^2, is defined for these measurements as

$$L^2 = D_{eff}/\Sigma_{a_{eff}} \tag{16}$$

The effective diffusion coefficient for the cell, D_{eff}, is given by

$$\frac{1}{D_{eff}} = \sum_i \frac{d_i v_i}{D_i} \tag{17}$$

where d_i is the flux disadvantage factor, $\bar{\Phi}_i/\bar{\Phi}_{cell}$; v_i is the volume fraction; and D_i is the diffusion coefficient of the i^{th} region or material. The effective absorption cross section of the cell, $\Sigma_{a_{eff}}$, is given by

$$\Sigma_{a_{eff}} = \sum_i d_i v_i \Sigma_{a_i} \tag{18}$$

where d_i and v_i are the same as for Equation 17, and Σ_{a_i} is Westcott's Maxwellian-averaged cross section for the i^{th} region and material. The values of D_i and Σ_{a_i} are given in Table V.

TABLE V

Thermal[a] Cross Sections for f and L^2 Analysis

	Natural U	Al	D_2O	H_2O
Σ_a	0.3163	0.0125	0.0000337	0.0197
Σ_s[b]	0.397	0.0850	0.464	3.191
D^{-1}[c]	1.4441	0.2568	1.192	6.536

(a) 20°C
(b) For computation of D^{-1}
(c) D^{-1} (mixture) = $\frac{\text{mol \% } D_2O}{0.839} + \frac{\text{mol \% } H_2O}{0.153}$

EXPERIMENTAL AND ANALYTICAL TECHNIQUES

The experimental disadvantage factors required to determine f and L^2 were obtained from measurements of the thermal neutron flux distribution. The technique consisted of irradiating both cadmium-covered and bare P-metal pins in representative positions in each lattice cell to obtain a subcadmium activation profile. It was assumed that the cutoff energy (0.554 ev) as determined for foils in an isotropic flux was applicable to the pins.

In the fuel the pins were loaded into specially drilled fuel segments 0.5 inch high as shown in Figure 4. No cadmium-covered pins were placed in the fuel. Instead, cadmium-covered pins were placed either directly on the cladding of a fuel rod or very near to it and the cadmium-covered activations were assumed to be constant through the fuel. The moderator traverses were made in two directions from the fuel cluster. The first traverse was directed toward an adjacent fuel assembly and the second at an angle of 30° from the first as shown in Figure 4. The cadmium-covered pins were set in holes in a light aluminum bar at 2-cm intervals. The bar was in turn clamped to the fuel rod. The bare pins were held in a very thin-walled aluminum tube drilled, on a diameter, to hold the pins at 1.00-cm spacings. These tubes were suspended from the cadmium traverse bar by a light nylon cord so that the pins would be at the same level as the pins in the fuel segments. A typical schematic is shown for a single rod in Figure 1.

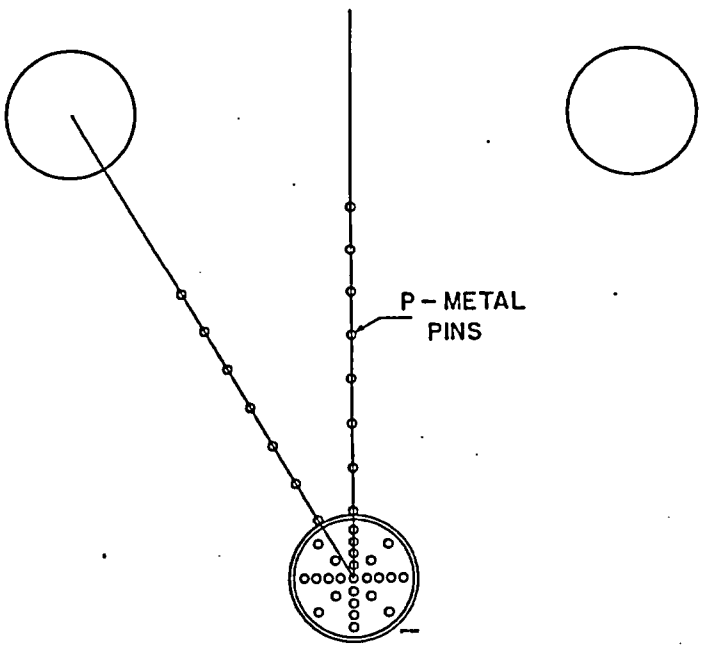

FIG. 4 SCHEMATIC OF PIN LOADINGS FOR f and L^2 MEASUREMENTS

The pins were counted on the standard 2x2-inch NaI(Tl) crystals with an integral bias discrimination of 0.5 Mev. The recorded counts were corrected for background, pin weight, and decay during the counting period. Each pin was counted a minimum of two times and the results were averaged. The average pin activations were then corrected for the overall pile flux distribution: i.e., a J_o correction radially and cosine correction vertically.

The corrected epicadmium activations were then plotted as a function of radial position in the cell and a smooth curve was drawn through the data. The appropriate epicadmium activation as determined from the curve was then subtracted from each bare pin activation. The resultant subcadmium activations in the moderator, i.e., exterior to the fuel cluster, were then plotted as a function of radial position. A smooth curve was again drawn through the data. These plots are shown in the Appendix for both the subcadmium and epicadmium activations. The average activation in the moderator, $\bar{\Phi}_M$, for each lattice was determined by numerical integration with a five-point Gaussian quadrature. The average activation in the fuel was determined by one of the following methods. In the case of a fuel rod that had azimuthal symmetry, viz, the single rod or central rod of the 7- and 19-rod clusters, the method followed that used in the moderator. In the other cases a contour plot of the subcadmium activations was constructed and the average activations were determined with a planimeter. The average subcadmium activations for the multirod clusters were then determined by weighting the individual rod averages by the fraction of each type of rods in the cluster.

The average activation in the aluminum cladding and in the D_2O coolant was obtained from the P-3 approximation to transport theory. The flux distributions were calculated for a cylindrical microcell composed of a single fuel rod with its associated cladding and coolant. Results were normalized to the average pin activations in the cluster. Comparisons of the calculated flux levels in the cladding with extrapolations of the measured subcadmium activations in the fuel gave good agreement. Measurements made by activating pins in various coolant position in the 19-rod cluster gave flux values slightly higher (Table VI) than the calculated values. Since the effect of this disagreement on the calculations of L^2 was negligible, the calculated values were retained for the other rod clusters.

The average relative activations for each region are given in Table VI. Initial values of f and L^2 were obtained directly from these numbers for the moderator purity at the time of the measurement. The results were then corrected to a moderator purity of 99.75 mol % D_2O. The corrections were made by use of the P-3 approximation.

TABLE VI

Relative Subcadmium Activations

Rods per Cluster	Lattice Pitch, inches	$\bar{\phi}_{F-1}$(a)	$\bar{\phi}_{F-2}$	$\bar{\phi}_{F-3}$	$\bar{\phi}_{F-4}$	$\bar{\phi}_{fuel}$	$\bar{\phi}_{Al}$	$\bar{\phi}_{coolant}$	$\bar{\phi}_{mod}$
1	7.00	1.000	-	-	-	-	1.22	-	1.815
	8.08	1.000	-	-	-	-	(1.23)	-	1.865
	9.33	1.000	-	-	-	-	1.23	-	1.916
	12.12	1.000	-	-	-	-	(1.23)	-	2.016
3	7.00	1.000	-	-	-	-	1.23	(1.31)	2.154
	9.33	1.000	-	-	-	-	(1.23)	(1.31)	2.302
	12.12	1.000	-	-	-	-	1.2	(1.31)	2.497
	14.00	1.000	-	-	-	-	(1.23)	(1.31)	2.608
7	9.33	0.706	1.049	-	-	1.000	(1.23)	(1.31)	2.689
	12.12	<0.703>	<1.049>	-	-	1.000	(1.23)	(1.31)	<3.233>
	14.00	0.697	1.051	-	-	1.000	1.22	(1.31)	3.229
	18.52	0.696	1.051	-	-	1.000	1.24	(1.31)	3.794
	21.00	<0.685>	1.053	-	-	1.000	(1.23)	(1.31)	3.902
7(b)	18.52	0.724	1.046	-	-	-	1.21	(1.40)	3.236
19	14.00	0.360	0.576	1.185	1.346	1.000	1.26	1.38	4.294
	18.52	0.398	0.574	1.077	1.449	1.000	1.26	1.38	5.150

(a) See Figure 2 for key to fuel rod indexing
(b) 2.0" center-to-center rod spacing in cluster
( ) Values used based on P-3 calculation
< > Values used inferred from foil data normalized to pin data

RESULTS

The results of the f and L^2 determinations are given in Table IX. They are also plotted in Figures 5 and 6. These plots serve both as a consistency test of the data and as a means of interpolating a value of f and L^2 for the 7-rod cluster at the 12.12-inch pitch, the data for which were unusable due to a loading error.

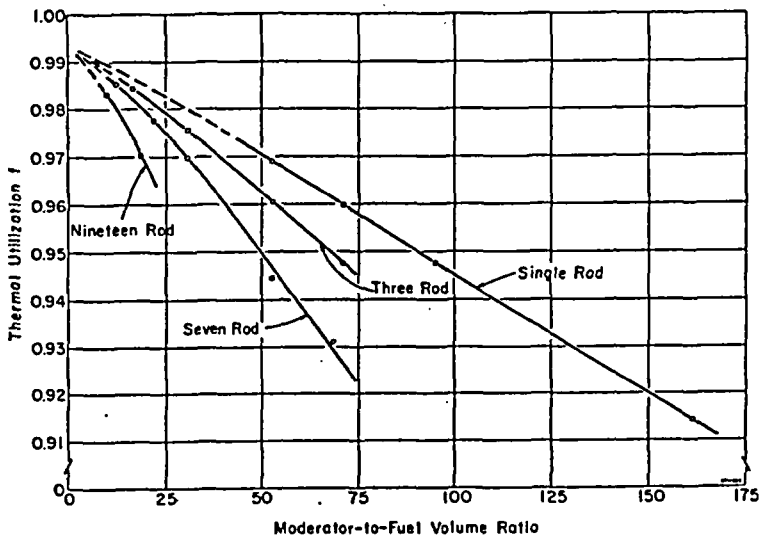

FIG. 5 EXPERIMENTAL VALUES OF THERMAL UTILIZATION VS MODERATOR-TO-FUEL VOLUME RATIOS

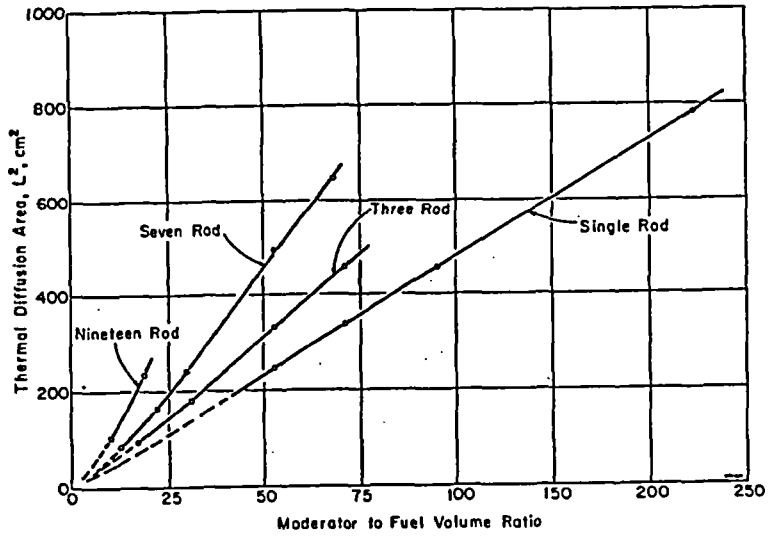

FIG. 6 EXPERIMENTAL THERMAL DIFFUSION AREA VS MODERATOR-TO-FUEL VOLUME RATIO

The absolute error to be associated with the L^2 results is largely dependent on the errors to be associated with the various cross sections, which in turn depend on the neutron spectrum assumed in obtaining the cross sections. The error in f is not very dependent on spectrum effects but is limited by the error in relative activation ratios. The standard deviation in the experimental activations as determined from statistical considerations is of the order of ±2% in L^2 and ±0.2% in f. Consequently an absolute error of ±3% in L^2 and ±0.2% in f is not unreasonable if the uncertainty in the cross sections is also taken into account. This error analysis does not account for systematic errors other than cross section errors.

RESONANCE ESCAPE PROBABILITY

THEORY OF THE MEASUREMENT

The resonance escape probability, p, for the natural uranium lattices under study is defined as the probability that a neutron entering the resonance energy region will escape capture in U^{238}. The model of neutron economy used in making this definition consistent with the other lattice parameter definitions is shown below.

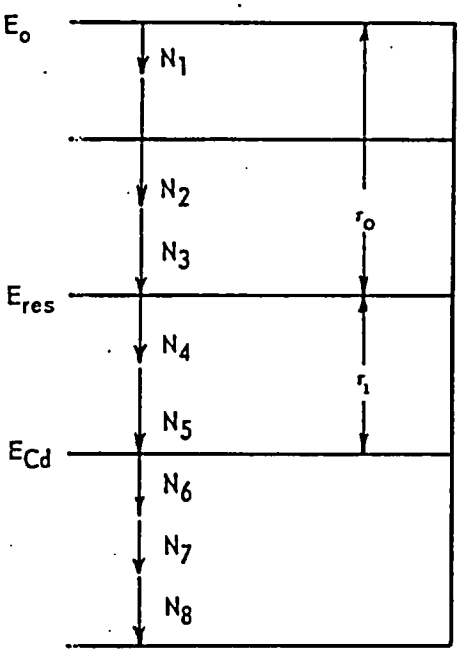

To enter the diagram, let N_1 be the number of neutrons resulting from U^{235} fissions. These neutrons are assumed to be at some effective fission neutron energy E_o. Then let N_2 be the effective number of neutrons produced by the fuel including fast fission. (Note that in agreement with the definition used earlier for ϵ, U^{238} captures are assumed not to take place in this region). Thus

$$\frac{N_2}{N_1} = \epsilon \tag{19}$$

Let N_3 be the number of neutrons reaching the resonance energy region, i.e., those escaping fast leakage, then

$$\frac{N_3}{N_2} = \frac{1}{1 + \tau_o B^2} \tag{20}$$

where τ_o is the neutron age to the resonance energy and B^2 is the buckling.

Let N_4 be the number of neutrons which slow down past the resonance region, then

$$\frac{N_4}{N_3} = p^{28} \tag{21}$$

where p^{28} is the resonance escape probability as defined above.

Let N_5 be the number of neutrons which slow down to an energy equal to the effective cadmium cutoff energy. This region between E_{res} and E_{cd} is generally referred to as the epicadmium 1/v region in that over this energy range both U^{238} and U^{235} are considered to have an absorption cross section which varies as 1/v. In this region neutrons may be absorbed or leak out; hence

$$\frac{N_5}{N_4} = \frac{p_{1/v}}{1 + \tau_1 B^2} \tag{22}$$

where $p_{1/v}$ is the probability of escaping capture in the 1/v region, and τ_1 is the neutron age from resonance to cadmium cutoff energy, which, within our definitions is the age from resonance to thermal energy.

Let N_6 be the number of neutrons escaping leakage by thermal diffusion prior to capture in the lattice, so that

$$\frac{N_6}{N_5} = \frac{1}{1 + L^2 B^2} \tag{23}$$

where L^2 is the thermal diffusion area.

Let N_7 be the number of neutrons captured thermally in U^{238} and U^{235}, and N_8 be the number captured thermally in U^{238} only. Then

$$\frac{N_7}{N_6} = f \tag{24}$$

where f is the thermal utilization, and

$$\frac{N_8}{N_7} = \frac{\Sigma_a^{28}}{\Sigma_a^{28} + \Sigma_a^{25}} \equiv F \tag{25}$$

where Σ_a^{238} and Σ_a^{235} are, respectively, the macroscopic cross sections of U^{238} and U^{235} in the thermal region.

The quantities ρ and $R_{1/v}$ are defined, consistent with our treatment of ϵ, as follows

$$\rho = \frac{\text{all } U^{238} \text{ epiCd captures}}{U^{238} \text{ subCd captures}} \tag{26}$$

and

$$R_{1/v} = \frac{\text{1/v epiCd captures in } U^{238}}{\text{subCd captures in } U^{238}} \tag{27}$$

The quantity ρ is directly measurable, while $R_{1/v}$ is inferred from cadmium ratio measurements with U^{235}. Thus

$$\rho - R_{1/v} = \frac{U^{238} \text{ resonance captures}}{U^{238} \text{ subCd captures}} \tag{28}$$

Referring to the neutron economy model,

$$\begin{aligned}
\rho - R_{1/v} &= \frac{N_3 - N_4}{N_8} \\
&= \frac{(1 - p^{28})N_3}{N_8} \\
&= (1 - p^{28}) \frac{N_3}{N_4} \frac{N_4}{N_5} \frac{N_5}{N_6} \frac{N_6}{N_7} \frac{N_7}{N_8} \\
&= (1 - p^{28}) \left(\frac{1}{p^{28}}\right) \left(\frac{1 + \tau_1 B^2}{p_{1/v}}\right) (1 + L^2B^2) \left(\frac{1}{f}\right) \left(\frac{1}{F}\right)
\end{aligned} \tag{29}$$

and solving for p^{28}

$$\frac{1 - p^{28}}{p^{28}} = \frac{(\rho - R_{1/v}) f F p_{1/v}}{(1 + L^2B^2)(1 + \tau_1 B^2)} \tag{30}$$

The values f, L^2, and B^2 have been measured. The value of the cross section ratio F can be determined from the Westcott cross sections given in Table VII.

TABLE VII

Cross Sections Used in p Analysis

Material	Thermal Absorption Cross Sections, barns
U^{235}	668.0
U^{238}	2.715

The value of τ_1 was numerically calculated for D_2O from the following

$$\tau_1 = \int_{\text{Cd cutoff}}^{30.\text{ev}} \frac{1}{3(\xi\Sigma_s)\Sigma_{tr}} \frac{dE}{E} \approx 26 \text{ cm}^2 \qquad (31)$$

where it is assumed that all resonance captures occur at 30 ev. The derivation of $p_{1/v}$ is similar to that for p^{28}. From the definition of $p_{1/v}$,

$$\frac{1 - p_{1/v}}{p_{1/v}} = \frac{\text{Absorptions in 1/v region}}{\text{No. entering thermal region}} \qquad (32)$$

$$= \frac{\text{1/v absorptions in } U^{238} + \text{1/v absorptions in } U^{235}}{\text{No. entering thermal region}}$$

Now

$$\text{No. 1/v absorptions in } U^{235} = \text{epiCd absorptions in } U^{235} \times \frac{\text{subCd absorption in } U^{235}}{\text{subCd absorption in } U^{235}}$$

$$= \frac{\text{epiCd fission in } U^{235} \times (\Sigma_a^{25}/\Sigma_f^{25})_{\text{epiCd}}}{\text{subCd fission in } U^{235} \times (\Sigma_a^{25}/\Sigma_f^{25})_{\text{subCd}}} \times \text{subCd absorption in } U^{235}$$

$$\equiv \frac{R_{25}(\Sigma_a^{25}/\Sigma_f^{25})_{\text{epiCd}}}{(\Sigma_a^{25}/\Sigma_f^{25})_{\text{subCd}}} \times \text{subCd absorptions in } U^{235} \qquad (33)$$

Now assuming $\nu^{25}_{\text{thermal}} = \nu^{25}_{\text{epiCd}}$ then

$$\kappa \equiv \frac{(\Sigma_f^{25}/\Sigma_a^{25})_{\text{subCd}}}{(\Sigma_f^{25}/\Sigma_a^{25})_{\text{epiCd}}} \approx \frac{(\eta^{25})_{\text{thermal}}}{(\eta^{25})_{\text{epiCd}}} \approx \frac{2.07}{1.74} = 1.19 \qquad (34)$$

by Westcott's formulation[5], for a cadmium thickness of 0.020 inch.

$$\text{No. 1/v absorptions in } U^{235} = (R_{25}\kappa) \times \text{thermal absorption in } U^{235} \qquad (35)$$

Similarly,

$$\text{No. 1/v absorptions in } U^{238} = R_{1/v} \times \frac{\text{thermal absorptions in } U^{235}}{(\Sigma_a^{25}/\Sigma_a^{28})_{\text{subCd}}} \qquad (36)$$

Now the total number of thermal events is a sum of the subcadmium absorption in U^{238}, U^{235}, and other materials, i.e., cladding and moderator, plus the leakage. This can be written

$$\text{Total No. entering thermal region} = \text{subCd absorption in } U^{235} \times \frac{\left[\Sigma_a^{25} + \Sigma_a^{28}\right]}{\Sigma_a^{25}} \left(\frac{1}{f}\right)(1 + L^2B^2) \qquad (37)$$

Combining Equations 32, 35, 36, and 37, one obtains

$$\frac{1 - p_{1/v}}{p_{1/v}} = \frac{\left[R_{25}\kappa + R_{1/v}(\Sigma_a^{28}/\Sigma_a^{25})\right]}{\left[\frac{\Sigma_a^{25} + \Sigma_a^{28}}{\Sigma_a^{25}}\right]\left[\frac{1 + L^2B^2}{f}\right]} \qquad (38)$$

The determination of $R_{1/v}$ is not made directly but is inferred from the U^{235} cadmium ratio. The following derivation indicates how this is accomplished.

$$R_{1/v} = \frac{\text{1/v epiCd captures in } U^{238}}{\text{subCd captures in } U^{238}} \qquad (27)$$

Assuming that U^{235} fission cross section varies as 1/v in both the subcadmium and epicadmium regions (an assumption for which a correction will be discussed), then

$$R_{1/v} = R_{25} = \frac{\text{No. } U^{235} \text{ epiCd fission}}{\text{No. } U^{235} \text{ subCd fission}} \tag{39}$$

Let A_{Cd} denote the measure of the fission production of a cadmium-covered U^{235} foil and A_B the fission product activity of an uncovered U^{235} foil then

$$R_{25} = \frac{A_{Cd}}{A_B - A_{Cd}} = \frac{1}{CR^{25} - 1} \tag{40}$$

where CR^{25} is the cadmium ratio of U^{235}. Hence

$$R_{25} = (CR^{25} - 1)^{-1} \tag{41}$$

Since the U^{235} cross section does not vary exactly as 1/v, a correction is necessary. The correction was evaluated using Westcott's energy spectrum and his tabulated cross sections. The value determined, using 0.020-inch cadmium and assuming the effective cadmium cutoff to be 0.554 ev, was

$$R_{1/v} = 0.94R_{25} \tag{42}$$

Hence we can write

$$\frac{1 - p_{1/v}}{p_{1/v}} = \frac{R_{25}\left[\kappa + 0.94(\Sigma_a^{28}/\Sigma_a^{25})\right]}{\left[\frac{\Sigma_a^{25} + \Sigma_a^{28}}{\Sigma_a^{25}}\right]\left[\frac{1 + L^2B^2}{f}\right]} \tag{43}$$

The other measurable quantity, ρ, which is defined by Equation 26, can be determined from the measure of activity of bare and cadmium-covered U^{238} foils. The basis for the determination of ρ used for these experiments was a measure of the activity induced by neutron capture of U^{238} according to the reaction

$$U^{238}(n,\gamma)U^{239} \xrightarrow[23 \text{ min}]{\beta,\gamma} Np^{239} \xrightarrow[2.3 \text{ days}]{\beta,\gamma} Pu^{239}$$

These measurements used the Np^{239} 2.3-day γ activity. Consequently, Equation 26 becomes

$$\rho = \frac{Np^{239} \text{ epiCd activity}}{Np^{239} \text{ subCd activity}} \tag{44}$$

Thus resonance escape probability can be calculated from the measured quantities R_{25}, f, L^2, B^2, and ρ according to Equation 30.

EXPERIMENTAL PROCEDURE

The determination of R_{25} (from which $R_{1/v}$ was determined), utilized the U^{235} fission product activities measured in the η experiment. The determination of f and L^2 was discussed in the previous section, while the B^2 determination is given in Reference 2.

The determination of ρ was made by irradiating paired sets of foils in representative fuel rods in the lattice. Each such set consisted of a natural uranium foil and a uranium foil depleted in U^{235} individually sandwiched between aluminum catcher foils ~0.001 inch thick. A natural uranium spacer 0.125 inch thick was used between the natural and depleted foils and between the foils and the top and bottom of a cadmium pill box. Table II gives the physical properties of the foils. All uranium faces in contact with the foils were machined flat so that any edge effects due to slightly rounded corners were negligible. The foil sets, one bare and one covered with cadmium 0.020 inch thick, were placed in the designated rods through windows cut in the cladding so that the rods and foils were aligned axially, as shown in Figure 1. The aluminum cladding was slightly deformed in the region of the cadmium-covered foil packet to allow for the presence of the cadmium. After the foils had been irradiated, they were allowed to cool for approximately two days in order to maximize the ratio of Np^{239} activity to fission product activity. The foils were then counted with a γ scintillator (NaI(Tl) activated) 2 inches wide and .4 mm thick coupled to a single-channel analyzer. Counting was performed over a "window" approximately 25 kev wide centered at 103 kev. The desired activities to be measured included the K_α X-rays of Pu (approximately 99 and 100 kev) resulting from the internal conversion following the β decay of Np^{239} plus the 106-kev γ ray from Np^{239} itself. However there was also some fission product background including 97-kev U internal conversion X-rays. The use of the two foils, in each set, of different U^{235} content permitted the determination of this background. A third set of foils, which consisted of an unirradiated foil of each type, was counted to determine the fraction of the measured activity which was due to the natural activity of the uranium.

A special measurement was made to determine an attenuation correction that must be applied to the counting data to account for the differences in the thickness of the natural

and depleted foils. This correction is necessary because of the high mass absorption coefficient of uranium for the γ and Pu X-rays being counted. The attenuation correction C is defined by

$$\frac{N_N}{N_D} = C \frac{A_N}{A_D} \tag{45}$$

where A_D and A_N are the measured activities of a depleted and a natural foil of different thickness, and N_D and N_N are the activities that would be obtained if there were no γ-ray attenuation. The value of C was determined experimentally in the following manner. First a measure of N counts was obtained from an irradiated uranium foil. Then an unirradiated natural uranium foil for which the natural activity was known was placed on top of the source foil shielding it from the crystal. This system was counted and the natural activity of the shielding foil subtracted giving N_N counts. The measure was repeated using a depleted foil which has a different thickness giving N_D. Then assuming

$$N_N = Ne^{-\mu t_N} \quad \text{and} \quad N_D = Ne^{-\mu t_D} \tag{46}$$

where μ is the mass absorption coefficient and t_D and t_N are the thickness of the depleted and material foil respectively, it can be shown that the attenuation correction becomes

$$C = \frac{1 - \frac{N_D}{N}}{1 - \left(\frac{N_D}{N}\right)^{t_N/t_D}} \times \frac{t_N}{t_D} \tag{47}$$

or that

$$C = \frac{1 - \left(\frac{N_N}{N}\right)^{t_D/t_N}}{1 - \frac{N_N}{N}} \times \frac{t_N}{t_D} \tag{48}$$

Both Equations 47 and 48 were used and an average of the two results was used for the correction factor.

The irradiated foils were counted alternately at least four times and in a sequence such that a simple average was sufficient to account for the time decay. The averaged counts were then divided by the weight of the foil. The natural

activity of the foils was subtracted and the foil attenuation correction applied. The fission product activity corrections were determined as shown in the following derivation of ρ from the measured activity.

Let A_N = measured activation of a bare natural uranium foil corrected as above

A_D = measured activation of a bare uranium foil depleted in U^{235} corrected as above

E_N^{25} = fraction of U^{235} in natural uranium foil

E_D^{25} = fraction of U^{235} in depleted uranium foil

Γ^{28} = measured γ activity per atom due to fission in U^{238}

Γ^{25} = measured γ activity per atom due to fission in U^{235}

Γ^{39} = measured γ activity per atom due to captures in U^{238} resulting in Np^{239}

The measured activity in the foils can then be written as

$$A_N = (1 - E_N^{25})\Gamma^{28} + E_N^{25}\Gamma^{25} + (1 - E_N^{25})\Gamma^{39}$$

$$A_D = (1 - E_D^{25})\Gamma^{28} + E_D^{25}\Gamma^{25} + (1 - E_D^{25})\Gamma^{39} \qquad (49)$$

Solving simultaneously for Γ^{25},

$$\Gamma^{25} = \frac{(1 - E_N^{25})A_D - (1 - E_D^{25})A_N}{(1 - E_N^{25})E_D^{25} - (1 - E_D^{25})E_N^{25}} \qquad (50)$$

Now the fission product activity due to U^{235} fission in the depleted foil, A_D^{25}, is given by

$$A_D^{25} = E_D\Gamma^{25} = \frac{E_D^{25}\left[(1 - E_N^{25})A_D - (1 - E_D^{25})A_N\right]}{(1 - E_N^{25})E_D^{25} - (1 - E_D^{25})E_N^{25}} \qquad (51)$$

The fast fission product γ activity of a bare depleted foil is found from the equation

$$A_D^{28} = \alpha A_D^{25} \qquad (52)$$

where A_D^{25} is as given in Equation 51, and α is the ratio of U^{238} fission product γ activity to U^{235} fission product γ

activity. The value of α is obtained from the following

$$\alpha = \frac{\delta}{P(t \rightarrow 2 \text{ to } 3 \text{ days})} \simeq \frac{\delta}{P(t \rightarrow \infty)} \qquad (53)$$

where δ is that obtained from the measurement of ϵ and $P(t \rightarrow \infty)$ was measured and found to be approximately unity. The resulting value of α is probably good within a factor of 2. The lack of accuracy in the value of α does not impair the accuracy of the ρ measurement since ρ is relatively insensitive to α.

The cadmium-covered foil activities are corrected for fission product activity in the following manner. The fission product activity due to epicadmium fissions in U^{235} is obtained from

$$A_D^{25}(\text{epiCd}) = \frac{A_D^{25}}{CR^{25}} \qquad (54)$$

where CR^{25} is the measured U^{235} cadmium ratio. The fission product activity from U^{238} is assumed to be all epicadmium so

$$A_D^{28}(\text{total}) = A_D^{28}(\text{epiCd})$$

The Np X-ray activity is given by

$$A^{39}(\text{total}) = A_D - (A_D^{25} + A_D^{28})$$

$$A^{39}(\text{epiCd}) = A_D(\text{epiCd}) - [A_D^{25}(\text{epiCd}) + A_D^{28}] \qquad (55)$$

from which ρ is computed according to the following equation

$$\rho = \frac{A^{39}(\text{epiCd})}{A^{39}(\text{total}) - A^{39}(\text{epiCd})} \qquad (56)$$

In the case of multiple rods the Np activities given by (55) for each rod are averaged over the cluster and

$$\rho^{28} = \frac{\overline{A^{39}(\text{epiCd})}}{\overline{A^{39}(\text{total})} - \overline{A^{39}(\text{epiCd})}} \qquad (57)$$

RESULTS

The measured values of ρ^{28} and $\overline{\rho^{28}}$ for the experimental lattices are given in Table VIII. The experimental values of CR^{25} are also given in the same table. The corresponding results for p are given in the last column of the table. These numbers have all been corrected to a moderator purity of 99.75 mol % D_2O by a calculation technique described elsewhere[12]. Although somewhat empirical, this computation is believed to be sufficiently accurate for calculations of small differences in moderator purity encountered in this series of experiments. The over-all standard deviation for the measurements is about 1% in p, including statistical errors. The principal systematic error is probably due to the effect of the cadmium depression on resonance energy neutrons, as a result of the suppression of thermal fissions. Preliminary investigations of this effect indicate that p^{28} values reported here may be high by approximately 1%.

TABLE VIII

Results of ρ^{28} and p^{28} Measurements

Rods per Cluster	Lattice Pitch, inches	D_2O, mol %	CR^{25} Rod 1	Rod 2	Rod 3	Rod 4	$\overline{CR^{25}}$	ρ^{28} Rod 1	Rod 2	Rod 3	Rod 4	$\overline{\rho^{28}}$	p^{28}(c)
1	7.00	99.70	42	-	-	-	42	0.181	-	-	-	0.181	0.956
	8.08	99.70	63	-	-	-	63	0.132	-	-	-	0.132	0.968
	9.33	99.70	82	-	-	-	82	0.114	-	-	-	0.114	0.972
	12.12	99.69	112	-	-	-	112	0.086	-	-	-	0.086	0.979
	Isolated	99.74	116	-	-	-	116	0.075	-	-	-	0.075	-
3	7.00	99.70	19	-	-	-	19	0.538	-	-	-	0.538	0.869
		99.51(a)	16	-	-	-	16	0.560	-	-	-	0.560	0.866
	9.33	99.71	33	-	-	-	33	0.336	-	-	-	0.336	0.916
		99.46(a)	26	-	-	-	26	0.322	-	-	-	0.322	0.921
	12.12	99.71	45	-	-	-	45	0.212	-	-	-	0.212	0.948
		99.55(a)	35	-	-	-	35	0.250	-	-	-	0.250	0.940
	14.00	99.70	48	-	-	-	48	0.242	-	-	-	0.242	0.941
		99.58(a)	41	-	-	-	41	0.233	-	-	-	0.233	0.944
	Isolated	99.74	48	-	-	-	48	0.205	-	-	-	0.207	-
7	9.33	99.71	12	15	-	-	15	0.913	0.635	-	-	0.662	0.843
	12.12	99.76	17	24	-	-	23	0.621	0.437	-	-	0.457	0.889
	14.00	99.76	19	28	-	-	27	0.554	0.383	-	-	0.401	0.902
	18.52	99.75	20	32	-	-	30	0.508	0.329	-	-	0.347	0.917
	21.00	99.75	21	33	-	-	31	0.507	0.336	-	-	0.354	0.916
	Isolated	99.74	21	33	-	-	31	0.568	0.347	-	-	0.368	-
7(b)	18.52	99.73	32	44	-	-	42	0.490	0.321	-	-	0.339	0.916
19	14.00	99.72	6	7.5	13	17	12	1.955	1.485	0.805	0.752	0.949	0.788
	18.52	99.73	7	10	19	21.5	17						
		99.19(a)	7	9.4	15	19	14	1.80	1.26	0.662	0.508	0.733	0.825
	Isolated	99.74	8	12	22	24	19	1.777	1.235	0.614	0.514	0.712	-

(a) Remeasured in Exponential Facility
(b) 2.0" center-to-center rod spacing in cluster
(c) See Figure 2 for key to fuel rod indexing
(d) Corrected to moderator purity at 99.75 mol % D_2O

The results shown for the three-rod cluster at the larger pitches indicate an error in one of the measurements. Also, in the buckling analysis, discussed in the next section, the results for the 3-rod cluster were somewhat worse than would be expected considering all the other data. Consequently, a series of remeasurements were made in an exponential facility. The 19-rod cluster at 18.52-inch lattice pitch was also measured at this time to fill a gap in the earlier data. The results for these measurements are given in Table VIII. These remeasurements matched the previous measurements within the experimental error and indicate the reproducibility of the experiments to be approximately 1/2%. However the remeasurements are probably to be preferred since they show the expected increase in p with increasing lattice pitch.

During the period these experiments were in progress, a flux trap was constructed in the PDP for a measurement of the resonance flux distribution from a line source[13]. This flux trap consisted of a central region of D_2O, with a radius of 114 cm, in a critical lattice. A fuel assembly placed in the center of this region could then be considered "isolated" as far as resonance events were concerned, i.e., to be coupled to the rest of the reactor only through the thermal flux. A measurement of ρ was made in this lattice for each of the four fuel assembly types, thus giving the limiting value of ρ as the moderator-to-fuel volume ratio tends to infinity. The results for each of these assembly types is shown in Figure 7.

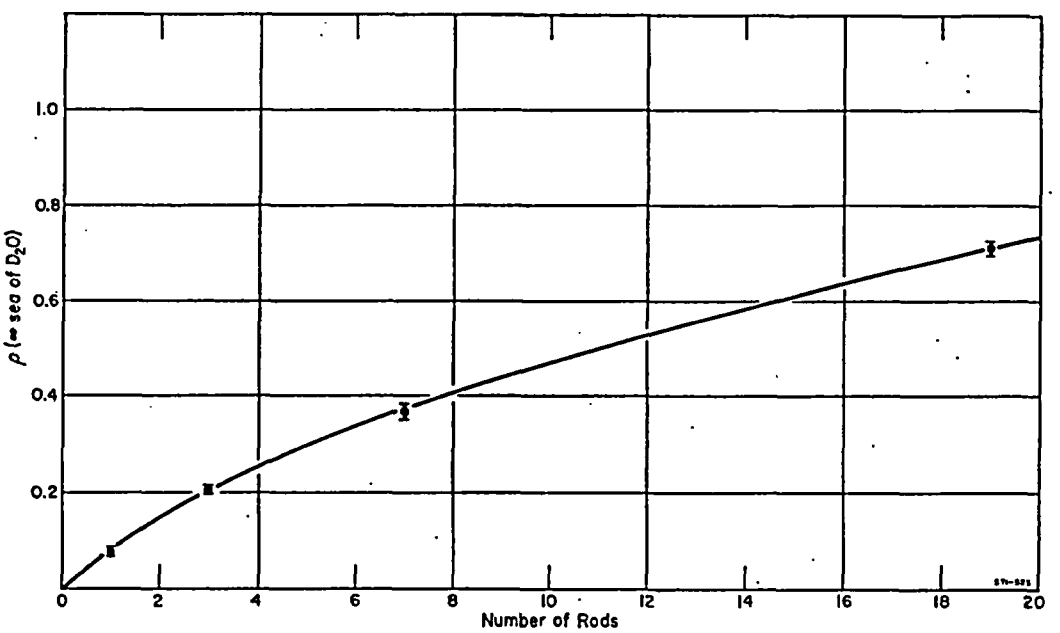

FIG. 7 ρ^{28} FOR AN ISOLATED ASSEMBLY VS NUMBER OF RODS IN THE ASSEMBLY

NEUTRON AGE

The neutron age or slowing down area, τ, was not measured directly for the lattices under consideration. However, a series of measurements were made to determine the age in pure moderator. These measurements were taken in the flux trap arrangement mentioned in the preceding section, and consisted of foil activations to determine the slowing down distribution at the indium resonance (1.46 ev) from a line source. A description of the experiment has been given by Graves[13]. The age-to-indium resonance corrected to pure D_2O was

$$\tau_{1.46\ ev} = 111\ cm^2$$

in good agreement with earlier determinations. For the age from 1.46 ev to thermal (Cd cutoff), a calculated value was used.

$$\tau_{1.46\ ev\ to\ thermal} = 8\ cm^2$$

Then

$$\tau_{thermal} = 119\ cm^2$$

for pure D_2O. Corrections for H_2O contamination were based on studies by Wade[14] which indicate the age decreases linearly by 4 cm^2 as the purity of the moderator changes from 100 to 99 mol % D_2O.

Values of τ for the experimental lattices were calculated from the moderator values. It was assumed that the scattering cross sections of the uranium and the moderator are approximately equal and that scattering from aluminum is negligible. Also it was assumed that the slowing down power of the uranium and aluminum are negligible compared to that of D_2O. With these assumptions it can be shown that

$$\frac{\tau(\text{lattice})}{\tau(\text{moderator})} \simeq \frac{V_T^2}{V_M(V_M + V_F)} \qquad (58)$$

where V_T is the lattice cell cross-sectional area, and V_M and V_F are the cross-sectional areas of the moderator and fuel, respectively. The computed values for τ are given in Table IX.

TABLE IX

Summary of Results of Cell Measurements and a Comparison of Bucklings Determined from Cell Measurements with Those Determined by Pile Flux Profile Method

Rods per Cluster	Lattice Pitch, inches	η[a]	ϵ[a]	p	f	CR^{25}	L^2, cm^2	τ,[b] cm^2	Bucklings[c] B_1^2, m^{-2}	B_2^2, m^{-2}	Difference $B_1^2 - B_2^2$, m^{-2}	% Difference $\frac{B_1^2 - B_2^2}{B_2^2}$
1	7.00	1.316	1.039	0.956	0.969	42	247	121	6.82	6.48	0.34	5.2
	8.08			0.968	0.960	63	336	120	5.62	5.29	0.33	6.2
	9.33			0.972	0.948	82	456	120	4.32	4.08	0.24	5.9
	12.12			0.979	0.914	112	783	119	2.42	2.30	0.12	5.2
3	7.00	1.314	1.048	0.866[d]	0.984	19	95	128	7.58	7.59	-0.01	-0.1
	9.33			0.921[d]	0.976	33	181	122	7.56	7.11	0.45	6.3
	12.12			0.940[d]	0.961	45	331	120	5.24	5.05	0.19	3.8
	14.00			0.943[d]	0.948	48	459	120	3.93	3.81	0.12	3.1
7	9.33	1.310	1.053	0.843	0.985	15	86	129	6.49	6.02	0.47	7.8
	12.12			0.889	0.978[f]	23	164[f]	124	6.57	6.11	0.46	7.5
	14.00			0.902	0.970	27	242	123	5.41	5.20	0.21	4.0
	18.52			0.917	0.945	30	496	121	3.07	2.92	0.15	5.1
	21.00			0.916	0.931	31	648	120	2.24	2.10	0.14	0.7
7[e]	18.52	1.313	1.044	0.916	0.947	42	418	121	3.43	3.26	0.17	5.2
19	14.00	1.311	1.077	0.788	0.983	12	106	133	3.82	3.41	0.41	12.0
	18.52			0.825	0.970	14	236	127	3.77	3.02	0.75	24.8

(a) Averaged for the cluster
(b) $\tau = \tau_0 + \tau_1$ and $\tau_1 = 26\ cm^2$ (see text)
(c) B_1^2 determined from cell measurements by three-group critical equation

$$\eta\epsilon pf\left(\frac{p_{1/v}CR^{25}}{CR^{25} - 1}\right) = (1 + L^2B^2)(1 + \tau_0B^2)(1 + \tau_1B^2)$$ and

$p_{1/v}$ is computed from CR^{25} (see text);

B_2^2 = flux profile measured bucklings (see Ref. 2)

(d) Remeasurements in Exponential (see text on resonance escape probability)
(e) 2.00" center-to-center rod spacing in cluster
(f) Interpolated from Figures 5 and 6

COMPARISON OF CELL PARAMETERS AND LATTICE BUCKLINGS

A particularly interesting test of the data obtained in these experiments can be made by comparing bucklings derived from the cell parameters given in this report with the separately measured lattice bucklings previously reported[2] Bucklings were obtained from the cell parameters by solving the three-group critical equation,

$$(1 + L^2B^2)(1 + \tau_0B^2)(1 + \tau_1B^2) = \eta\epsilon pf\frac{p_{1/v}CR^{25}}{CR^{25} - 1} \qquad (59)$$

Symbols have been defined in the previous sections. This critical equation is used instead of the usual four-factor, two-group equation in order to be consistent with the derivation of the resonance escape probability. It may be noted that the results given by the three-group equation differ from two-group results by less than 0.5% in reactivity.

The bucklings that were computed from the cell parameters are given in Table IX along with the measured lattice bucklings. The per cent deviation of the computed buckling from that measured is generally better than 8% with the majority of the cases within 6%. These deviations are consistently higher than would be expected from the experimental uncertainty. The higher computed bucklings indicate a systematic error exists in the cell measurements which has not been resolved.

T. J. Hurley, Jr.
T. J. Hurley Jr./ncp
Approved by

J. L. Crandall
J. L. Crandall, Research Manager
Experimental Physics Division

BIBLIOGRAPHY

1. Dunklee, A. E. "The Heavy Water System of the Process Development Pile". E. I. du Pont de Nemours & Co., Savannah River Laboratory, Aiken, S. C. USAEC Report DP-567 (1961); Baumann, N. P. "Process Development Pile Measurements of Lattice Parameters of Natural Uranium in Heavy Water". ibid. DP-407 (1959).

2. Hurley, T. J., Jr., H. R. Fike, and G. F. O'Neill. "Experimental Bucklings of Heavy Water Moderated Lattices of Natural Uranium Metal Rod Clusters". Nuclear Sci. and Eng. 12, No. 3 (1962).

3. Westcott, C. H., W. H. Walker, and T. K. Alexander. "Effective Cross Sections and Cadmium Ratios for the Neutron Spectra of Thermal Reactors". Proc. U. N. Intern. Conf. Peaceful Uses Atomic Energy, 2nd, Geneva, 16, 70-6 (1958). P/202

4. Hughes, D. J., et al. Neutron Cross Sections. Brookhaven National Laboratory. Upton, N. Y. USAEC Report BNL-325, 2nd Edition (1958), Suppl. 1 (1960).

5. Westcott, C. H. Effective Cross Section Values for Well-Moderated Thermal Reactor Spectra. Chalk River, Ontario, Canada, Report CRRP-960 (1960); CRRP-662 (1956); CRRP-680 (1957); CRRP-787 (1958), and CRRP-862 (1959).

6. Spinrad, B. I. "Fast Effect in Lattice Reactors". Nuclear Sci. and Eng. 1, 455-60 (1956).

7. Bondarenko, I. I., et al. "Average Number and Spectrum of Prompt Neutrons in Fast-Neutron-Induced Fission". Proc. U. N. Intern. Conf. Peaceful Uses Atomic Energy, 2nd, Geneva, 15, 353-60 (1958). P/2187

8. Safford, G. J. and W. W. Havens, Jr. "Fission Parameters for U^{235}". Nucleonics 17, No. 11, 134 (1959).

9. Futch, A. H., Jr. "Fast Fission Effect in Lattices of Natural Uranium and Heavy Water". Nuclear Sci. and Eng. 5, No. 1, 61-7 (1959).

10. Kinard, F. E. and N. P. Baumann. "Some Parameters Affecting Measurements of the Fast Fission Factor". American Nuc. Soc. Trans. 3, No. 1, 23 (1960).

11. Carter, M. D., A. J. Perks, and L. G. Sanders. The Measurements of U^{238}: U^{235} Fission Ratios. United Kingdom Atomic Energy Authority, Research Group, Atomic Energy Research Establishment, Harwell, Berks, England. Report AERE-R-3205 (1960).

12. Dessauer, G. "Physics of Natural Uranium Lattices in Heavy Water". Proc. U. N. Intern. Conf. Peaceful Uses Atomic Energy, 2nd, Geneva, 12, 320-40 (1958). P/590

13. Graves, W. E. "Measured Slowing Down Distribution at the Indium Resonance from a Line Source of Fission Neutrons in Heavy Water". Nuclear Sci. and Eng. 12, No. 3, (1962).

14. Wade, J. W. "Neutron Age in Mixtures of D_2O and H_2O". Nuclear Sci and Eng. 4, 12-25 (1958).

APPENDIX – PROFILES OF FOIL ACTIVATIONS

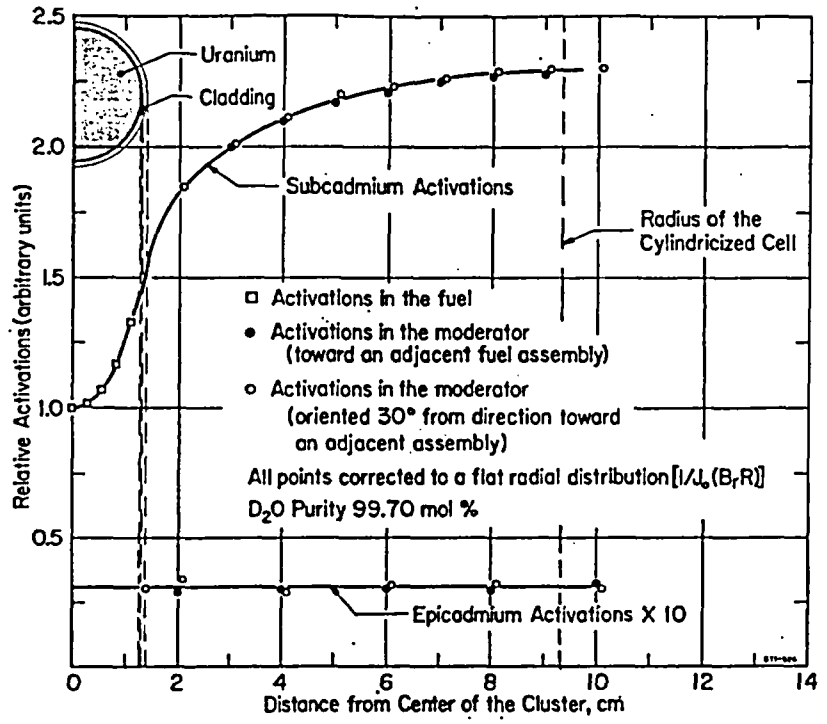

FIG. A-1 SINGLE ROD ON 7.00" PITCH

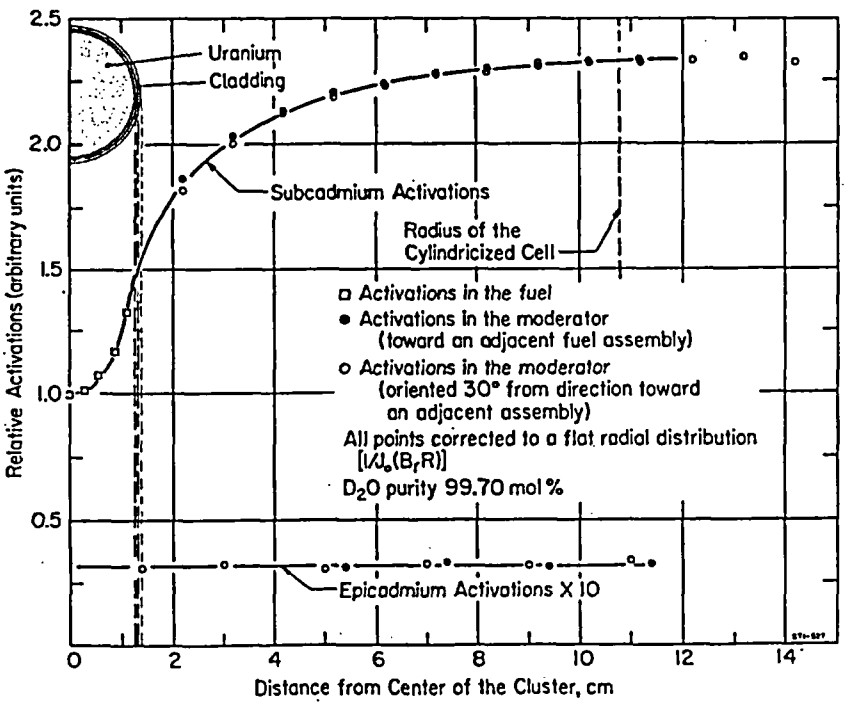

FIG. A-2 SINGLE ROD ON 8.08" PITCH

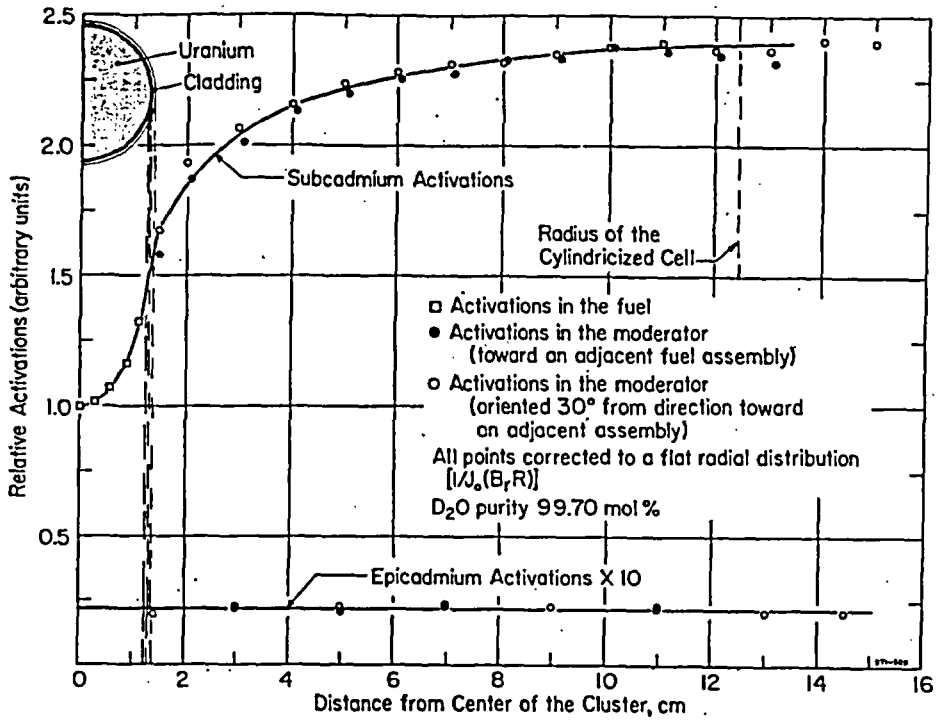

FIG. A-3 SINGLE ROD ON 9.33" PITCH

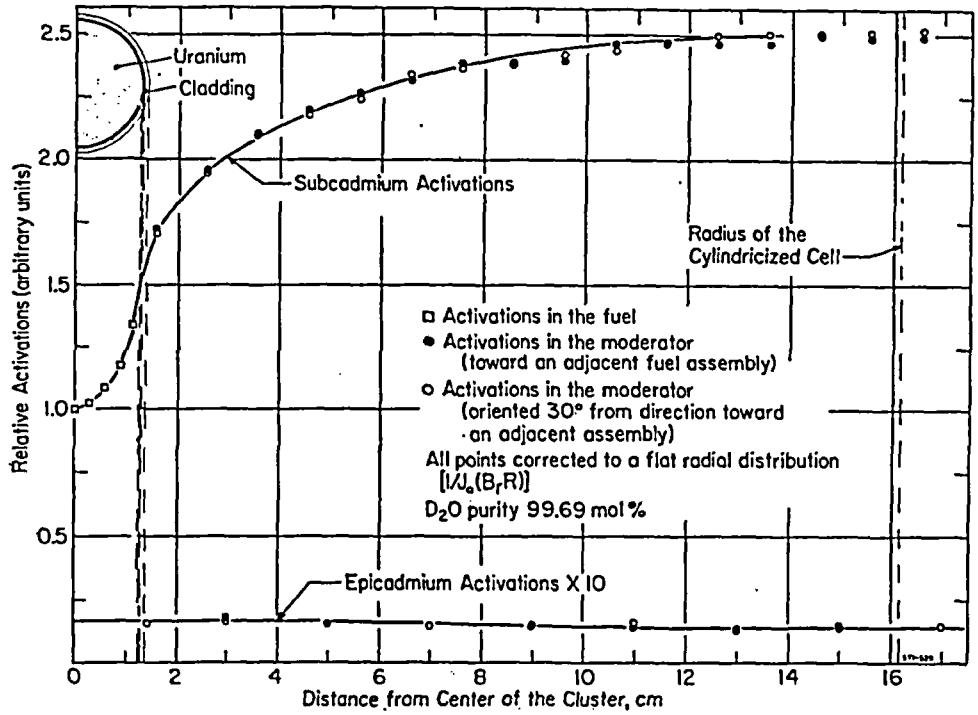

FIG. A-4 SINGLE ROD ON 12.12" PITCH

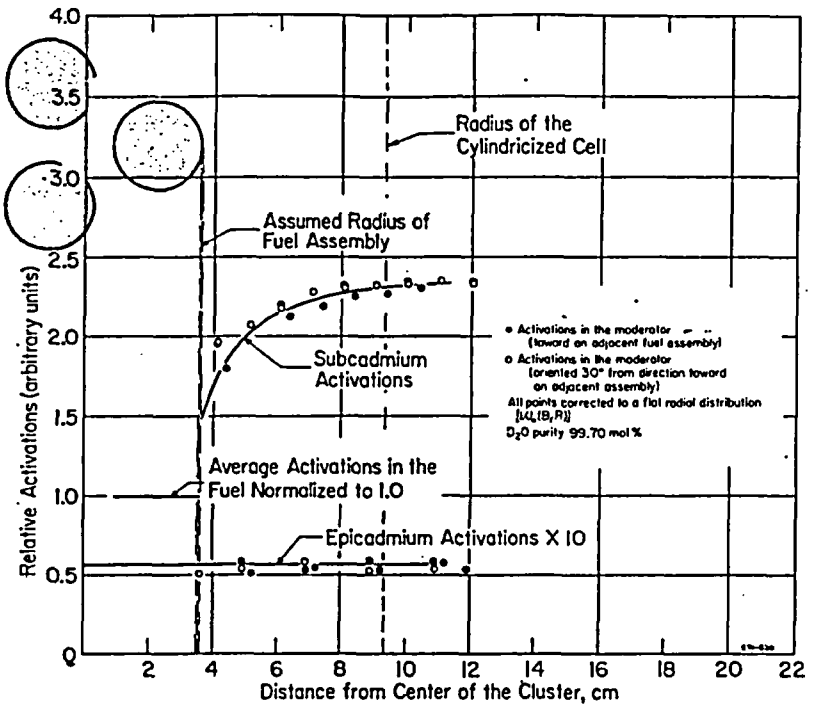

FIG. A-5 THREE-ROD CLUSTER 7.00" PITCH

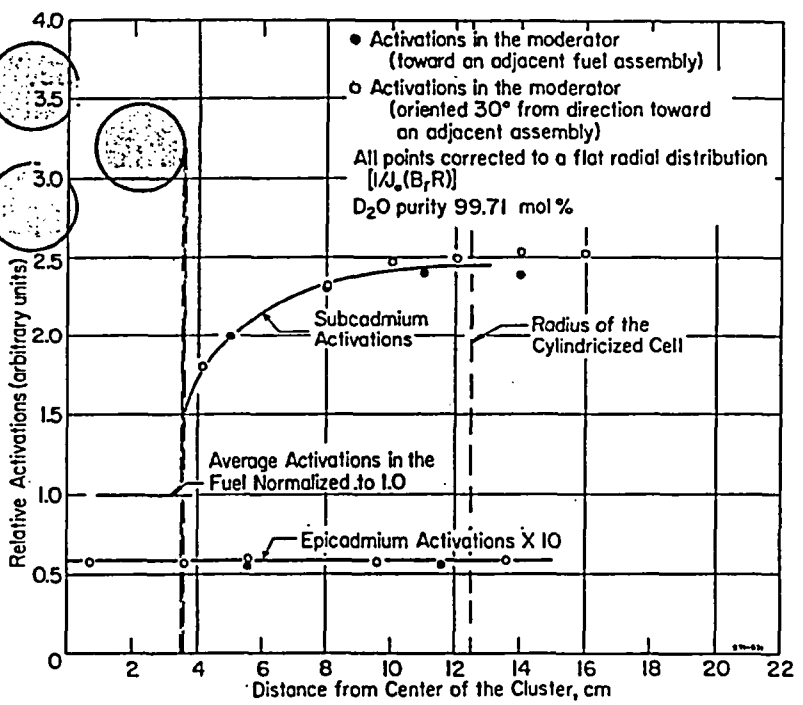

FIG. A-6 THREE-ROD CLUSTER 9.33" PITCH

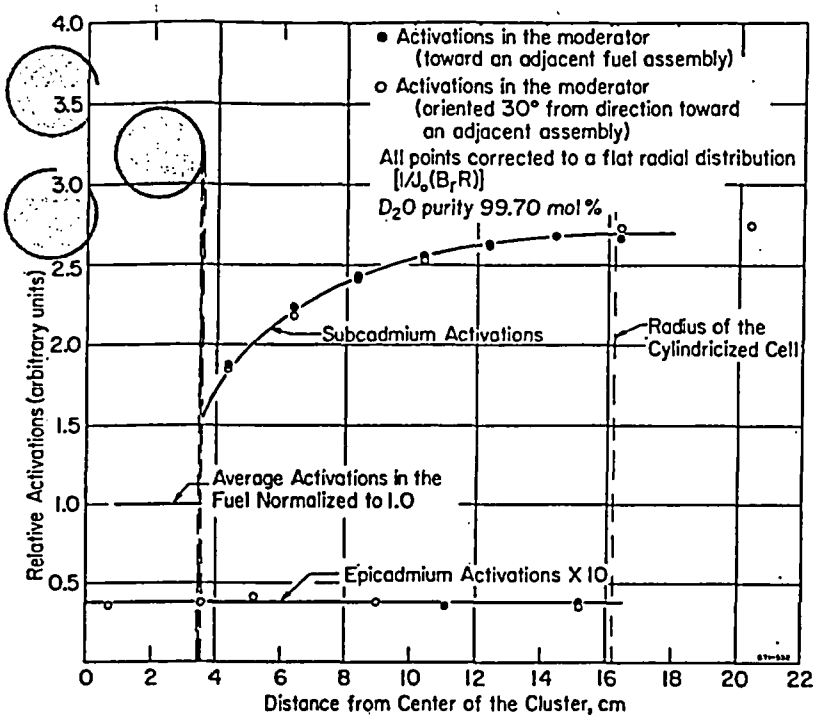

FIG. A-7 THREE-ROD CLUSTER 12.12" PITCH

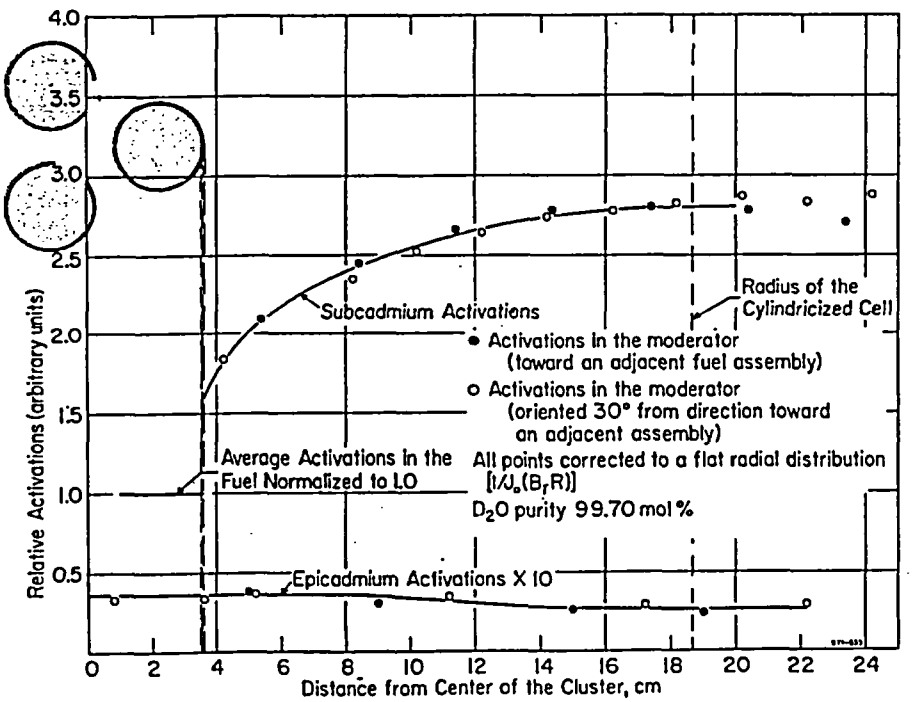

FIG. A-8 THREE-ROD CLUSTER 14.00" PITCH

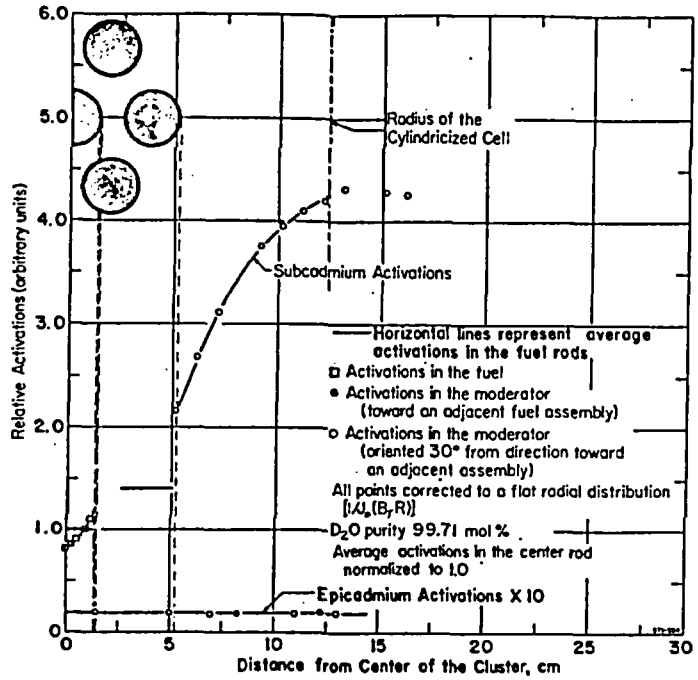

FIG. A-9 SEVEN-ROD CLUSTER 9.33" PITCH

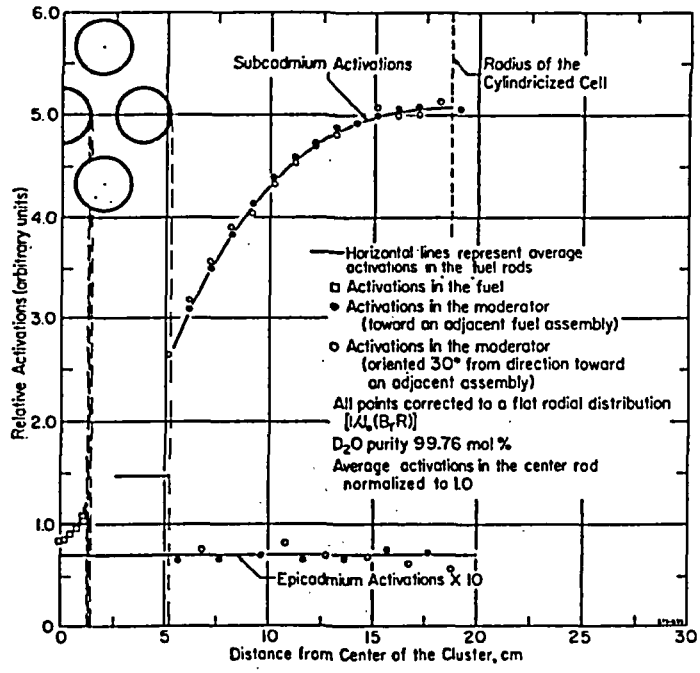

FIG. A-10 SEVEN-ROD CLUSTER 14.00" PITCH

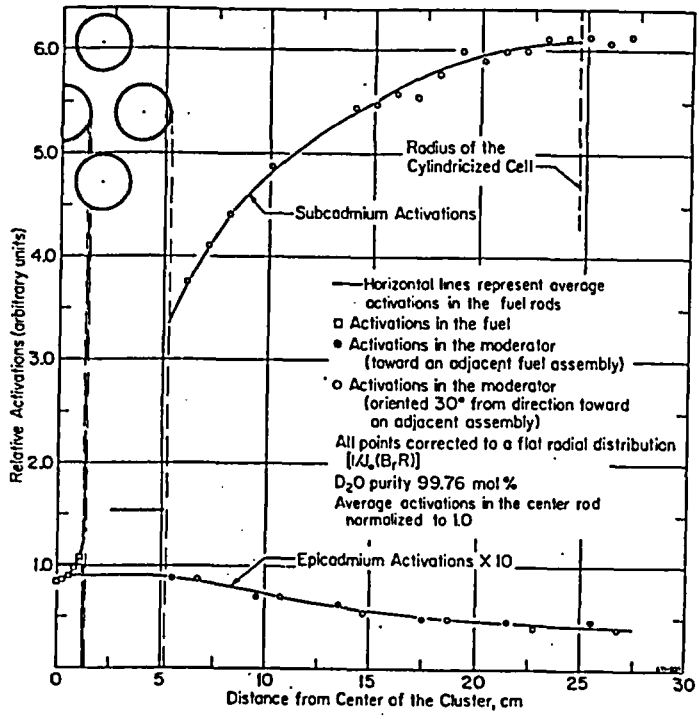

FIG. A-11 SEVEN-ROD CLUSTER 18.52" PITCH

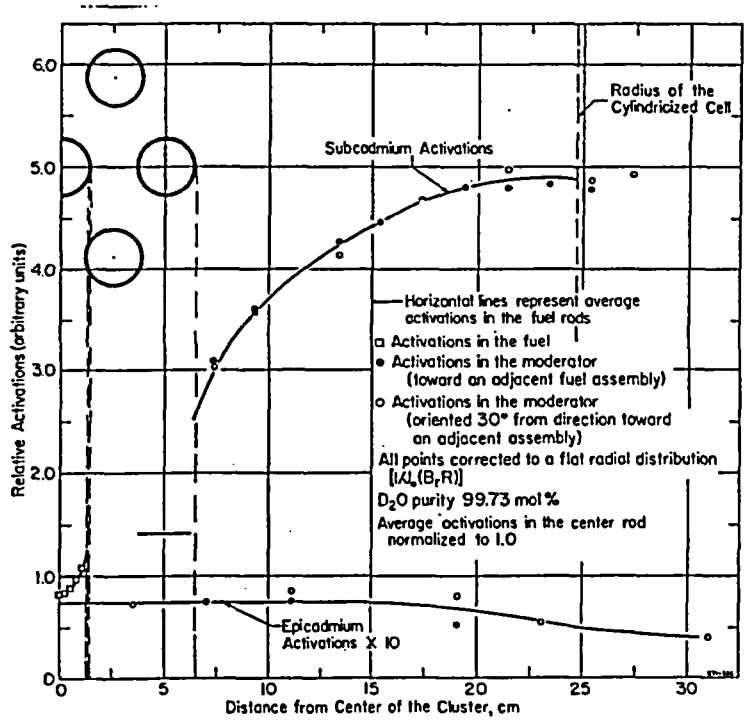

FIG. A-12 SEVEN-ROD CLUSTER 18.52" PITCH

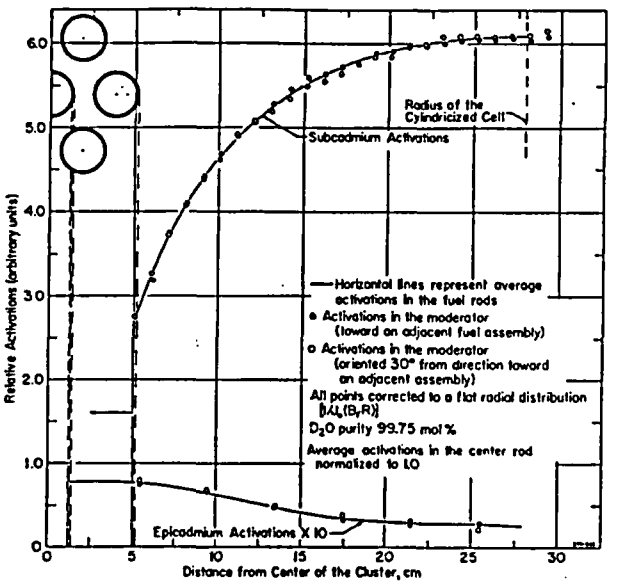

FIG. A-13 SEVEN-ROD CLUSTER 21.00" PITCH

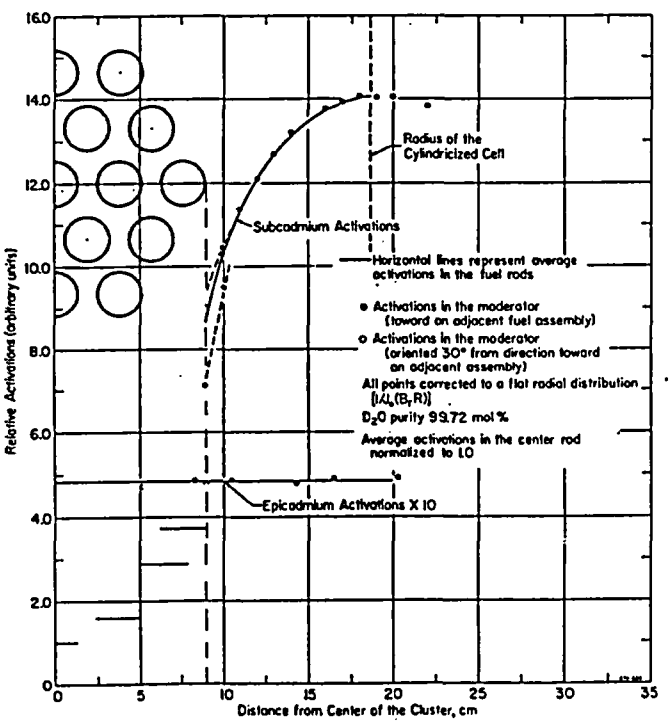

FIG. A-14 NINETEEN-ROD CLUSTER 14.00" PITCH

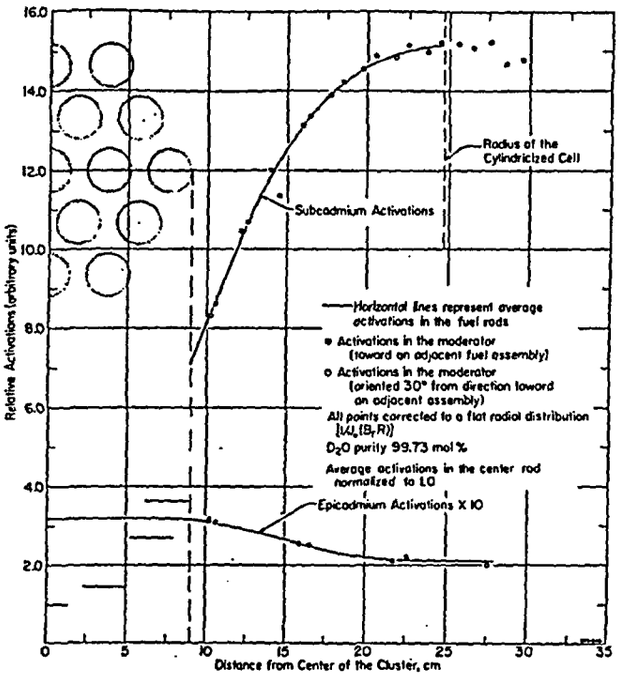

FIG. A-15 NINETEEN-ROD CLUSTER 18.52" PITCH